Intergranular corrosion of copper in the presence of benzotriazole

Aboubakr M. Abdullah, Faiza M. Al-Kharafi, Badr G. Ateya *

Chemistry Department, Faculty of Science, Kuwait University, B.O. 5969, Safat 13060, Kuwait

Abstract

While benzotriazole (BTAH, $C_6H_5N_3$) has long been known as an efficient inhibitor for the general corrosion of copper, this paper documents the occurrence of intergranular corrosion (IGC) of copper in a salt solution (3.5 wt.% NaCl) in the presence of 1 mM BTAH. This occurs above a breakdown potential, E_b, at the end of the passive region. Higher concentrations of BTAH broaden the passive region and shift E_b to more noble values. Pitting is the mode of corrosion above E_b in the presence of a higher concentration of BTAH, while IGC occurs above E_b in the presence of 1 mM of BTAH.
© 2006 Acta Materialia Inc. Published by Elsevier Ltd. All rights reserved.

Keywords: Copper; Benzotriazole; Intergranular corrosion; Pitting; Chloride

1. Introduction

The interaction of benzotriazole (BTAH) with the surfaces of copper and its alloys is a subject of considerable importance in connection with its use as a corrosion inhibitor. The subject has been extensively studied and the mechanisms of inhibition well documented. Two mechanisms have been proposed, postulating the formation of a polymeric film of Cu(I)–BTA [1–9] or an adsorbed layer of BTAH on the surface [1–3,10–16]. The above works dealt predominantly with the efficiency of BTAH as an inhibitor for the corrosion of copper and its alloys under free corrosion conditions.

The behavior of BATH and the stability of the protective film have not been explored at more noble potentials than that of free corrosion in laboratory tests. This is a particularly significant point in view of the fact that copper and its alloys are protected with BTAH in many service environments containing dissolved oxidants. Such oxidants raise the free corrosion potential significantly above the values normally measured in laboratory experiments.

Intergranular corrosion (IGC) of copper often received much less attention than some other forms of corrosion. This paper documents the occurrence of intergranular corrosion (IGC) of copper in an aqueous medium of 3.5 wt.% NaCl, which has the nominal salt level of sea water, in the presence of a low concentration of BTAH. In addition to the serious consequences of this phenomenon, which has not been recognized, chloride brines are particularly significant in connection with the extensive use of copper and its alloys in marine environments [17], refineries [18–20], and power generation [21] which are of particular importance to Kuwait and the Gulf region. Furthermore, some references in the literature suggest that lower concentrations of BTAH promote, rather than inhibit, the corrosion of copper [22,23], while many others point to a favorable effect of chloride ions on the stability and efficiency of the copper–BTAH complex [24–26].

2. Experimental

Electrodes were prepared from Cu (99.9%) obtained from Goodfellow. The Cu electrodes (disks of area $0.2\ cm^2$) were polished using SiC papers successively down to 2400 grits, followed by 0.3 μm alumina to acquire a mirror-like finish. A conventional three-electrode cell was

---

* Corresponding author. Tel.: +965 498 7453; fax: +965 4816482.
  E-mail address: ateya@kuc01.kuniv.edu.kw (B.G. Ateya).

used with a Ag/AgCl reference electrode, $E = 0.197$ V SHE, and a Pt sheet counter electrode. Solutions were prepared using deionized water, BTAH from Aldrich and NaCl from Fluka.

Potentiodynamic polarization curves (at a scan rate of 2 mV s^{-1}) and potentiostatic polarization curves (at selected potentials) were measured on Cu electrodes in 3.5 wt.% NaCl solutions containing 0, 10^{-3}, 5×10^{-3} and 10^{-2} M BTAH. Potential scanning was from less to more noble potentials. Measurements were performed at 25 ± 1 °C while the electrolyte was stirred using a magnetic stirrer without gas bubbling. The surfaces of the electrodes were examined using a scanning electron microscope (JSM-6300 JEOL).

All measurements were done while the solutions were open to air.

3. Results

The effect of BTAH on the polarization behavior of copper in 3.5 wt.% NaCl is shown in Fig. 1. BTAH has a strong inhibiting effect on the rate of anodic dissolution of copper. This inhibiting effects prevails throughout a passive region which extends from the free corrosion potential (-0.257 V Ag/AgCl) up to the breakdown potential, E_b. An increase in the concentration of BTAH shifts the breakdown potential, E_b, to more noble values. Beyond E_b, the current increases rapidly with potential (see curves b and c).

This inhibiting effect was also tested by measuring the current transients supported by copper electrodes upon being polarized at selected potentials within the passive region in the presence of various concentrations of BTAH. The current transients are shown in Fig. 2 while the SEM images are shown in Fig. 3. These images were taken after each specimen was polarized for 3 h at the chosen potential. Note the decrease in the current and in the extent of corrosion upon increase of the concentration of BTAH.
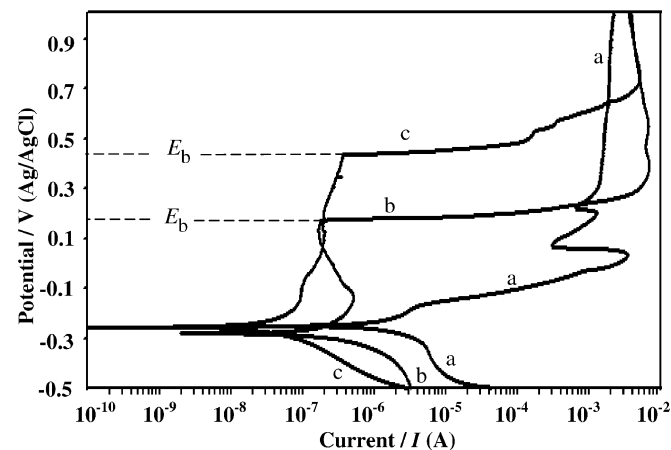

Fig. 1. Polarization curves of Cu electrodes in 3.5 wt.% NaCl in the presence of different concentrations of BTAH: (a) 0, (b) 1×10^{-3} and (c) 5×10^{-3} M. The break down potential, E_b is marked for curves b and c.
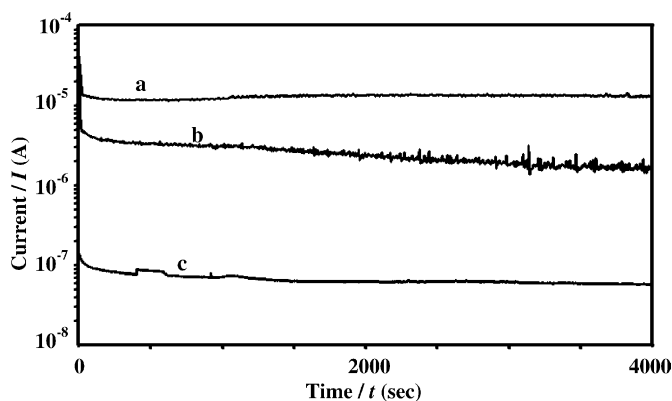

Fig. 2. Effect of the concentration of BTAH on the current transient supported by the copper electrodes (0.2 cm^2) polarized at (a) 0 V (Ag/AgCl) in 1×10^{-3} M BTAH, (b) 0.2 V (Ag/AgCl) in 5×10^{-3} M BTAH and (c) 0.2 V (Ag/AgCl) in 1×10^{-2} M BTAH. These potentials are in the middle of the passive region.
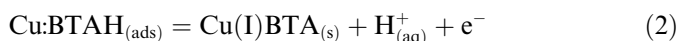
Other sets of current transients and SEM images were obtained at potentials above the breakdown potentials, E_b, in the presence of different concentrations of BTAH. The current transients are shown in Fig. 4 while the localized corrosion is documented by SEM images in Fig. 5(a)–(d). The images in Fig. 5(a)–(c) display intergranular corrosion at different locations of the surface that was polarized at 0.2 V (Ag/AgCl) in the presence of 10^{-3} M BTAH. On the other hand the images in 5d reveal the presence of pits (black spots in the circled regions) in the copper surface polarized at 0.6 V (Ag/AgCl) in the presence of 5×10^{-3} M BTAH.

4. Discussion

The anodic branch in the polarization curve (Fig. 1) shows a passive region that extends for about 0.4 V above the free corrosion potential. This region ends at a breakdown potential, E_b, which is about 0.176 V (Ag/AgCl) in the presence of 1×10^{-3} M BTAH. During this passive region, the anodic dissolution current decreases by about two orders of magnitudes in the presence of 1×10^{-3} M BTAH compared to the unprotected chloride medium (compare Fig. 1(a) and (b)). The inhibiting effect of BTAH in the passive region is attributed to the formation of the Cu(I)BTA complex via an adsorption process, i.e.

$$Cu_{(s)} + BTAH_{(aq)} = Cu{:}BTAH_{(ads)} + H^+_{(aq)} \tag{1}$$

where Cu:BTAH$_{(ads)}$ refers to BTAH adsorbed on the copper surface. Under oxidizing conditions, this adsorbed species can be oxidized to give the protective complex, i.e.

$$Cu{:}BTAH_{(ads)} = Cu(I)BTA_{(s)} + H^+_{(aq)} + e^- \tag{2}$$

Increasing the BTAH concentration shifts reactions 1 and 2 towards the formation of more of the protective complex Cu(I)BTA. This, in turn, shifts E_b to more noble values and hence broadens the passive region in the polarization
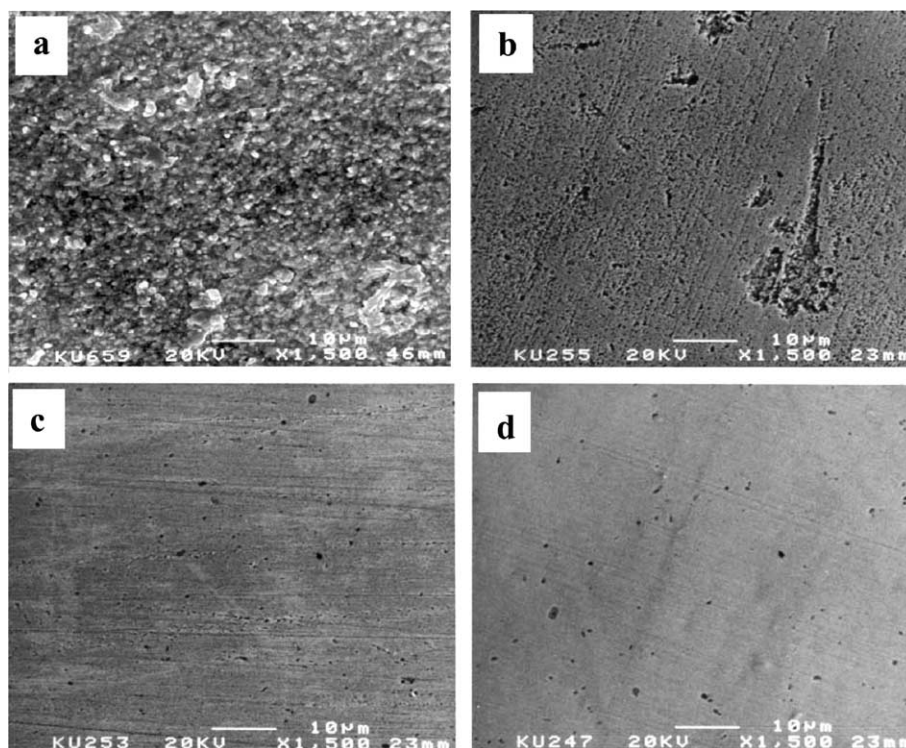
Fig. 3. SEM micrographs of Cu after being polarized in the 3.5% NaCl for 3 h under the following conditions: (a) 0 M BTAH at 0 V (Ag/AgCl), (b) 10^{-3} M BTAH at 0 V (Ag/AgCl), (c) 5×10^{-3} M BTAH at 0.2 V (Ag/AgCl) and (d) 10^{-2} M BTAH at 0.2 V (Ag/AgCl). The potentials in (b), (c) and (d) are in the middle of the passive region.
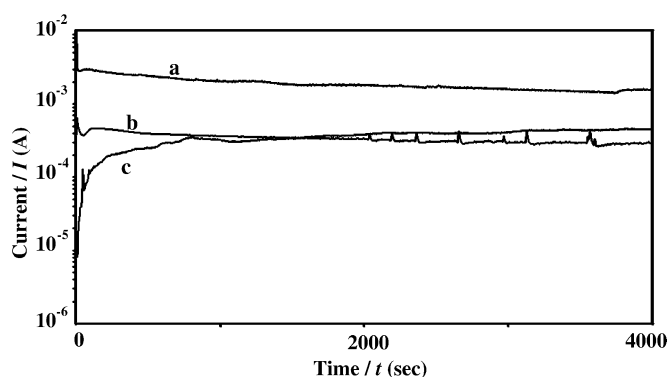

Fig. 4. Current transients of Cu electrodes polarized above the breakdown potential under the following conditions: (a) 10^{-3} M BTAH at 0.200 V (Ag/AgCl), $E_b = 0.176$ V Ag/AgCl, (b) 5×10^{-3} M BTAH at 0.600 V (Ag/AgCl) $E_b = 0.435$ V Ag/AgCl and (c) 10^{-2} M BTAH at 0.600 V (Ag/AgCl). $E_b = 0.435$ V Ag/AgCl.

curve. The value of E_b is 0.435 V (Ag/AgCl) for 5×10^{-3} M BTAH compared to 0.176 V (Ag/AgCl) in the presence of 10^{-3} M BTAH. Beyond the breakdown potential, the current increases rapidly with potential. This is attributed to localized corrosion which is documented by the SEM images presented below. The form of this localized corrosion depends on the concentration of BTAH as shown below.

An increase in the concentration of BTAH is associated with a decrease in the current in the passive region (Fig. 2) and a decrease in the extent of corrosion (Fig. 3). An order of magnitude increase in the concentration of BTAH (from 10^{-3} to 10^{-2} M) decreases the current in the passive region by about two orders of magnitude (compare curves a and c in Fig. 2). Note the frequent current spikes in curve b which are attributed to initiation and passivation of metastable pits. The absence of these spikes in curve c is a consequence of the high protection efficiency brought about by the high concentration of BTAH (10^{-2} M) which does not allow initiation of pits (see also Fig. 3(d)). Similar spikes exist in curve a although they are less visible in view of the differences in the (logarithmic) scale of the current.

The presence of BTAH has a profound effect on the extent of corrosion (see Fig. 3(a)–(d)). While Fig. 3(a) shows extensive general corrosion of the surface that was tested in the absence of BTAH, the images in (b), (c) and (d) show progressively lower extents of corrosion of the surface in the presence of 10^{-3}, 5×10^{-3} and 10^{-2} M BTAH, respectively. Some residual pits resist the inhibiting effects of BTAH at its highest concentration, as seen in the image (d). Such pits may account for the small current ($\sim$100 nA) provided by the electrode in the presence of 10^{-2} M BTAH (see curve in Fig. 2).

In Fig. 4, the Cu electrodes were polarized at potentials above the breakdown potentials, E_b, in the presence of various concentrations of BTAH. The steady current in the presence of 10^{-3} M BTAH is an order of magnitude greater than those measured in the presence of the higher
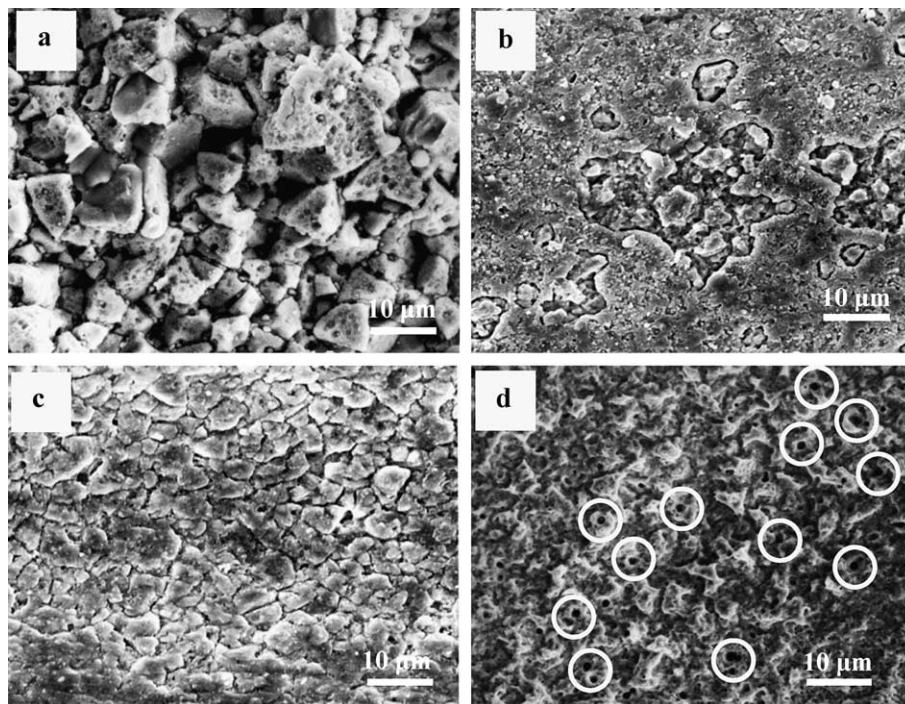
Fig. 5. SEM micrographs of Cu after being polarized in 3.5 wt.% NaCl for 3 h above the breakdown potential, E_b, under the following conditions: (a)–(c) intergranular corrosion in the presence of 10^{-3} M BTAH at 0.2 V (Ag/AgCl) and (d) pitting corrosion in the presence of 5×10^{-3} M BTAH at 0.6 V (Ag/AgCl). Images (a)–(c) are different regions of the same sample. The black spots inside the encircled regions in image (d) are attributed to pits.

concentrations of 5×10^{-3} and 10^{-2} M BTAH. This large current (curve a) is attributed to the extensive intergranular corrosion (IGC) that occurs in the presence of 10^{-3} M BTAH under a potential of 0.2 V (Ag/AgCl), see Fig. 5(a)–(c) which show various regions of the sample. This IGC occurred at a potential (0.2 V) that is only 0.024 V more noble than the breakdown potential which is 0.176 V (Ag/AgCl) in the presence of 1 mM BTAH.

On the other hand, Fig. 5(d) was obtained after the electrode was polarized at 0.6 V (Ag/AgCl) for 3 h in the presence of 5×10^{-3} M BTAH. This potential is more noble than the corresponding E_b (0.435 V Ag/AgCl). The prevailing mode of localized corrosion under this condition is not IGC but rather pitting corrosion. The locations of these pits are the black spots which are inside the white circles.

Intergranular corrosion is often attributed to the geometry of the tilted grain boundaries [27–29] and the segregation of impurities such as Ni, Sb and As [30,31] to this region. BTAH is known to be a highly efficient inhibitor for the corrosion of copper and much less efficient for other metals such as Ni [32] and Zn [33]. Hence, in view of the low concentration (1×10^{-3} M BTAH) and the low affinity of BTAH to adsorb on the grain boundary impurities, the amount of BTAH adsorbed onto the grain boundary regions is too small to protect it against corrosion.

5. Summary

Using electrochemical and surface characterization techniques, it is shown that benzotriazole (BTAH) passivates the surface of copper in 3.5% NaCl. The extent of this passivation increases with the concentration of BTAH. Beyond the passive region, the metal undergoes intergranular corrosion in the presence of 1 mM BTAH whereas it undergoes pitting corrosion in the presence of a higher concentration of BTAH.

Acknowledgements

References

[1] Chan HYH, Weaver MJ. Langmuir 1999;15:3348.
[2] Tornkvist C, Thierry D, Bergman J, Liedberg B, Leygraf C. J Electrochem Soc 1989;136:58.
[3] Fang B-S, Olson CG, Lynch DW. Surf Sci 1986;176:476.
[4] Poling GW. Corros Sci 1970;10:359.
[5] Youda R, Nishihara H, Aramaki K. Corros Sci 1988;28:87.
[6] Brusic V, Frisch MA, Eldridge BN, Novak FP, Kaufman FB, Rush BM, et al. J Electrochem Soc 1991;138:2253.
[7] Modestov AD, Zhou G-D, Wu Y-P, Notoya T, Schweinsberg DP. Corros Sci 1994;36:1931.
[8] Tromans D, Li G. Electrochem Solid State 2002;5:5.
[9] Jin-Hua C, Zhi-Cheng L, Shu C, Li-Hua N, Shou-Zhuo Y. Electrochim Acta 1998;43:265.
[10] Schultz ZD, Biggin ME, White JO, Gewirth AA. Anal Chem 2004;76:604.
[11] Polewska W, Vogt MR, Magnussen OM, Behm RJ. J Phys Chem B 1999;103:10440.

[12] Walsh JF, Dhariwal HS, Gutierrez-Sosa A, Finetti P, Muryn CA, Brookes NB, et al. Surf Sci 1998;415:423.

[13] Lewis G. Br Corros J 1981;16:169.

[14] Mansfeld F, Smith T, Parry EP. Corrosion 1971;28:289.

[15] Cho K, Kishimoto J, Hashizume T, Pickering HW, Sakurai T. Appl Surf Sci 1995;87–88:380.

[16] Tsirlin M, Eidelman A, Lesin S, Branover H. J Mater Sci Lett 1996;15:508.

[17] Kawabe A. Electrochemistry 2003;71:681.

[18] Garverick L. Corrosion in the petrochemical industry. ASM; 1994. p. 107.

[19] Vipper AB, Balak GM, Ponomarenko NA, Kalinin LL. Chemistry and technology of fuels and oils (Khimiya i Tekhnologiya Topliv i Masel) 1989;24:353.

[20] Keera ST, Eissa EA, Taman AR. Anti-Corros Meth M 1998;45: 252.

[21] Lin HHR. In: 1992 International joint power generation conference, October 18–22. New York: ASME; 1992. p. 19. 31.

[22] Frignani A, Tommesani L, Brunoro G, Monticelli C, Fogagnolo M. Corros Sci 1999;41:1205.

[23] Frignani A, Fonsati M, Monticelli C, Brunoro G. Corros Sci 1999;41:1217.

[24] Hashemi T, Hogarth CA. Electrochim Acta 1988;33:1123.

[25] Rubim JC, Gutz IGR, Sala O, Orville-Thomas WJ. J Mol Struct 1983;100:571.

[26] Biggin ME, Gewirth AA. J Electrochem Soc 2001;148:C339.

[27] Miyamoto H, Ikeuchi K, Mimaki T. Scripta Mater 2004;50:1417.

[28] Palumbo G, Aust KT, Lehockey EM, Erb U, Lin P. Scripta Mater 1998;38:1685.

[29] Kim SH, Erb U, Aust KT, Palumbo G. Scripta Mater 2001;44:835.

[30] Zhu Y, Mimura K, Isshiki M. Oxid Met 2003;59:575.

[31] Khaldeev GV, Knyazeva VF, Volyntsev AB, Spivak LV. Prot Met+ 1979;15:583.

[32] Cao PG, Yao JL, Zheng JW, Gu RA, Tian ZQ. Langmuir 2002;18:100.

[33] Fenelon AM, Breslin CB. J Appl Electrochem 2001;31:509.